On the Similarity between Cluster and Galactic Stellar Initial Mass Functions

Bruce G. Elmegreen

IBM Research Division, T.J. Watson Research Center, P.O. Box 218, Yorktown Heights, NY 10598, USA, bge@watson.ibm.com

ABSTRACT

The stellar initial mass functions (IMFs) for the Galactic bulge, the Milky Way, other galaxies, clusters of galaxies, and the integrated stars in the Universe are composites from countless individual IMFs in star clusters and associations where stars form. These galaxy-scale IMFs, reviewed in detail here, are not steeper than the cluster IMFs except in rare cases. This is true even though low mass clusters generally outnumber high mass clusters and the average maximum stellar mass in a cluster scales with the cluster mass. The implication is that the mass distribution function for clusters and associations is a power law with a slope of -2 or shallower. Steeper slopes, even by a few tenths, upset the observed equality between large and small scale IMFs. Such a cluster function is expected from the hierarchical nature of star formation, which also provides independent evidence for the IMF equality when it is applied on sub-cluster scales. We explain these results with analytical expressions and Monte Carlo simulations. Star clusters appear to be the relaxed inner parts of a widespread hierarchy of star formation and cloud structure. They are defined by their own dynamics rather than pre-existing cloud boundaries.

Subject headings: stars:formation — stars: mass functions — ISM: structure — galaxies: star clusters

1. Introduction

The initial mass function (IMF) for stars in star clusters is similar to the integrated IMF in whole galaxies, even though the integrated IMF is a sum from many clusters which themselves have a decreasing mass function. This observed similarity has been used to suggest that stellar mass is effectively independent of cluster mass (Elmegreen 2000, 2001), aside from the obvious condition that a cluster cannot produce a star more massive than itself. Without such independence, the relatively large number of low mass clusters would

overpopulate the field with purely low mass stars and tilt the integrated IMF to be steeper than the IMF inside each cluster.

Kroupa & Weidner (2003) turned the argument around, suggesting that the tendency for more massive clusters to contain more massive stars, which comes from statistical sampling, is enough to make the summed IMFs from all clusters steeper than the individual IMFs. Assuming a cluster mass function $dn_{cl}/dM_{cl} \propto M_{cl}^{-\beta}$ with a slope $\beta = 2.2$, they obtained a summed IMF with a slope of -2.8 when the intrinsic cluster IMF has a slope of about -2.35, the Salpeter value (see compilation of cluster IMFs in Scalo 1998; see review in Chabrier 2003). Correcting for 100% binaries steepened the summed IMF in Kroupa & Weidner (2003) to a slope of -3.2. With the further assumption that most stars form in clusters, they concluded that the IMF for whole galaxies should be much steeper than the Salpeter function. This conclusion has important consequences for integrated galaxy colors, metallicities, and supernova rates (see also Goodwin & Pagel 2005 for a discussion of the supernova rate).

This steepening of the integrated IMF for galaxies compared to the IMF for clusters depends sensitively on the cluster mass function (see Fig. 2 in Kroupa & Weidner 2003 and Sect. 3 below). In particular, the steepening is negligible for $\beta \lesssim 2$. To investigate β further, Weidner, Kroupa, & Larsen (2004) considered the correlation between maximum cluster luminosity, $L_{\rm cl,max}$, and galaxy star formation rate, SFR. This correlation has a lot of dispersion so the slope of the cluster mass function cannot be well constrained from the data alone. However, they note that $\beta = 2.35$ makes the formation time of a cluster population independent of the total cluster mass. This derived power of 2.35 is essentially one larger than the power in the observed correlation SFR $\propto L_{\rm cl,max}^{1.35}$. To obtain $\beta = 2.35$, the maximum cluster mass, $M_{\rm cl,max}$, was assumed to be proportional to the maximum cluster luminosity. Such a proportionality requires the maximum-mass clusters in each galaxy to have the same age, regardless of SFR. Larsen (2002) showed, however, that a cluster population with a uniform distribution of ages and a maximum cluster mass (limited by galaxy size, for example) has a luminosity function that is steeper than the mass function. In the case he considered, the luminosity function had a slope of -2.72 while the mass function had a slope of -2. The difference arises because the high luminosity clusters are systematically younger than than the low luminosity clusters, considering the cluster mass cutoff. Thus the slope of the cluster mass function derived by Weidner, Kroupa & Larsen (2004) should be considered an upper limit. If cluster mass functions are shallower than $\beta = 2.35$, then the difference between the integrated galaxy IMF and the cluster IMF is smaller than they suggest.

Weidner & Kroupa (2005) considered the additional influence of galaxy size. Small galaxies, which generally have low total star formation rates, should have fewer clusters and

a smaller maximum mass for their cluster populations, compared to large galaxies. Models with this effect and the cluster $\beta = 2.35$ suggested that dwarf galaxies should have steeper integrated IMFs than large galaxies, with slopes between -3.1 and -3.3 when individual cluster IMFs have the Salpeter slope. These authors also returned to the case where $\beta = 2.0$ (their Fig. 8), and again found a negligible effect on the summed IMF (i.e., a steepening in slope from the Salpeter value by only 0.1), even in the dwarf galaxy case.

The cluster mass function has been measured for several galaxies. Zhang & Fall (1999) observed $\beta \sim 1.95 \pm 0.03$ and $\beta = 2.00 \pm 0.08$ for young and old clusters respectively in the Antennae galaxy, which is the largest sample available for any galaxy. Another large sample is in recent HST data of M51, where Gieles et al. (2006) fitted the luminosity function to a mass function with $\beta = 2.0$ and an upper mass cutoff $\sim 10^5$ $M_\odot$. For the LMC, the nearest galaxy whose complete cluster population can be studied, Elmegreen & Efremov (1997) obtained $\beta \sim 2.0$ using clusters from Bica et al. (1996); Hunter, et al. (2003) obtained $\beta = 2$ to 2.4 in two different ways using clusters from Bica et al. (1999) with photometry from Massey (2002); and de Grijs & Anders (2006) obtained $\beta = 1.85 \pm 0.05$ using the same data as in Hunter et al. but different age calibrations. Other cluster studies of whole galaxies recently got similar β; for example de Grijs et al. (2003) found $\beta = 2.04 \pm 0.23$ for 147 massive clusters NGC 3310 and $\beta = 1.96 \pm 0.15$ for 177 clusters in NGC 6745. Larsen (2002) considered 6 nearby galaxies and derived luminosity functions with slopes of 2 to 2.4 but did not derive mass functions; most likely, the mass functions are shallower (see above). Evidently, $\beta \sim 2$ is not uncommon for cluster systems. This implies the IMF on galactic scales should be approximately equal to the individual cluster IMFs.

These theoretical predictions about the summed IMF should be compared with observations. Does the integrated IMF in galaxies have a slope as steep as -3? Do dwarf galaxies have steeper IMF slopes than large galaxies? If not, then how can we understand intuitively why integrated IMFs are approximately equal to individual cluster IMFs? In what follows, we begin with a more detailed discussion of the $\beta = 2$ case, and then we discuss the observations of summed IMFs in Section 3. Section 4 demonstrates some properties of summed IMFs using Monte Carlo simulations that include a soft rejection criterion for overly massive stars in a cluster. This criterion seems appropriate for clouds that form stars with an efficiency less than one. It also tends to make the summed IMF more similar to the individual cluster IMFs, even when $\beta > 2$.

2. Summed IMFs in the $\beta = 2$ case: An Intuitive Explanation

We consider in this section the special case where the cluster mass function is a power law with decreasing slope $\beta = 2$. We assume that this function applies to both clusters and loose stellar groupings, and that the stars in each have the same IMF.

Generally, the maximum stellar mass in a cluster, M_{max}, found on average from the equation

$$\int_{M_{max}}^{\infty} n_s(M)dM = 1 \tag{1}$$

for stellar IMF $n_s = n_{s0}M^{-1-x}$, is related to the normalization factor n_{s0} by the expression $n_{s0} = xM_{max}^x$ (Sect. 3 considers a more realistic IMF but gets the same result as in this discussion). Here the notation corresponds to $x = 1.35$ for the Salpeter IMF. The cluster mass is

$$M_{cl} = \int_{M_{min}}^{\infty} Mn_s(M)dM = n_{s0}M_{min}^{1-x}/\left(x-1\right) = n_{s0}/A, \tag{2}$$

where $A = (x-1)M_{min}^{x-1}$ is a constant. The cluster mass M_{cl} is proportional only to the IMF normalization factor n_{s0} and the fixed minimum stellar mass, $M_{\rm min}$. (In this paper, the notation will denote cluster mass by a subscript "cl.") Thus the number of stars in a cluster with a particular stellar mass range, M to $M + dM$, is directly proportional to the mass of the cluster:

$$n_s(M|M_{cl}) = AM_{cl}M^{-1-x}. \tag{3}$$

We use the notation for conditional probability, writing $n_s(M|M_{cl})$ for the IMF inside a cluster of mass M_{cl}.

Now consider the IMF for the sum of all clusters, $n_{sum}(M)$. This is given by the integral over the IMFs for each cluster of mass M_{cl}, weighted by the cluster mass function, $n_{cl}(M_{cl}) = n_{cl,0}M_{cl}^{-\beta}$:

$$n_{sum}(M) = \int_{M_{cl}(M_{max}=M)}^{M_{cl,max}} n_s(M|M_{cl})n_{cl}(M_{cl})dM_{cl} = AM^{-1-x}\int_{M_{cl}(M_{max}=M)}^{M_{cl,max}} n_{cl,0}M_{cl}^{1-\beta}dM_{cl}. \tag{4}$$

The lower limit to the integral is the cluster mass which has a maximum stellar mass equal to M, from equation 2,

$$M_{cl}(M_{max} = M) = xM^x/A. \tag{5}$$

This is a lower limit to the integral because only this cluster mass and larger cluster masses are likely to contain a star of mass M (on average). For $\beta = 2$, the integral in equation 4 is

$$n_{sum}(M) = An_{cl,0}M^{-1-x}\ln\left(AM_{cl,max}/xM^x\right). \tag{6}$$

This is essentially the same as the individual cluster IMF because the logarithmic function varies slowly with stellar mass M.

As an illustration of this point, suppose there are 100 clusters with masses between 10^2 and 10^3 $M_\odot$ and 10 clusters with masses between 10^3 and 10^4 $M_\odot$ (which follows from $\beta = 2$). The IMF normalization n_{s0} is proportional to cluster mass, so we set $n_{s0} = 1$ for the first interval and $n_{s0} = 10$ for the second. The summed IMF is the number of clusters times the IMF of each, which is $n_{s0}M^{-1-x}$, so the sum is $100M^{-1-x}$ for both intervals. This has the same overall mass dependence as the IMF in each cluster.

The reason low mass clusters do not tilt the summed IMF to significantly steeper slopes when $\beta \sim 2$ is that, with the above assumptions (Eq. 1), the probability of forming a star of a particular mass is independent of the cluster mass. The low M_{cl} bin has a low M_{max} *on average* because M_{max} scales with the cluster mass as $M_{max} \propto M_{cl}^{1/x}$ from equation 5. But there are 10 times more clusters with this low cluster mass than in the high mass bin, and in all of these additional clusters the actual maximum mass varies a lot around the average. In fact, there is likely to be one *extreme* example of a low-mass cluster with a maximum stellar mass that equals the *average* maximum mass in the higher cluster mass bin. Thus each bin of cluster mass has the same maximum stellar mass, and the same number of all other stellar masses.

We demonstrate this point using Monte Carlo simulations in Figure 1, below. A simple argument goes like this. Consider a cluster of mass M_{cl} which has the nominal or average maximum stellar mass given by equations 1 and 2, $M_{max} = (AM_{cl}/x)^{1/x}$. Now find the maximum stellar mass that is likely to occur, not in every cluster as assumed by equation 1, but once in some small fraction f of all the clusters with the same mass M_{cl}. This different maximum, $M_{max,f}$, is given by the equation

$$\int_{M_{max,f}}^{\infty} n_s(M)dM = f, \tag{7}$$

because the integral is the number of times the maximum $M_{max,f}$ occurs, and we are looking for a number that is the fraction of f the number of total clusters. Solving for $M_{max,f}$ with the same M_{cl} and therefore the same IMF normalization $n_{s0} = xM_{max}^x$, we get $M_{max,f} = M_{max}f^{-1/x}$. Now we ask: what is the cluster mass $M_{cl,f}$ which has $M_{max,f}$ as an *average* maximum mass? This comes from equation 5 and is

$$M_{cl,f} = xM_{max,f}^x/A = xM_{max}^x/\left(Af\right) = M_{cl}/f. \tag{8}$$

This result says that the *absolute* maximum stellar mass in $1/f$ clusters of mass M_{cl} is equal to the average maximum stellar mass in one cluster of mass M_{cl}/f. The numerical example

above took $f = 0.1$. This is true regardless of the cluster mass function slope β. It follows only from the power law nature of the IMF, regardless of the actual power x. The cluster mass function comes in when we realize that for $\beta = 2$, there are in fact $1/f$ clusters of mass M_{cl} for every one cluster of mass $M_{cl,f} = M_{cl}/f$.

The summed IMF is equal to the individual IMF also if $\beta < 2$, because then the integral in equation 4 depends only on the upper limit to the cluster mass, which is independent of M.

This derivation showing that the slope of the summed IMF is about equal to the slope of the individual IMF for $\beta \leq 2$ is independent of the IMF itself. Thus it applies to both the IMF slope for intermediate to high mass stars as well as the shallower slope for low mass stars.

Observations of galactic-scale IMFs are presented in the next section. They uniformly support this picture: the summed IMFs from all the clusters and dissolved clusters that ever lived is about the same as the average IMF in any one cluster. The implication is not that star formation samples clouds in a strange way, but only that the cluster mass function has a slope of $\beta \sim 2$, as observed directly in many cases.

This slope β is also suggested by the hierarchical nature of star formation itself. This structure is commonly observed on scales ranging from sub-parsec clusters to OB associations to kpc-size star complexes (see Elmegreen et al. 2006 and references therein). Very young, embedded clusters show this hierarchy of stellar positions too, as in Taurus (Gomez et al. 1993), NGC 2264 (Dahm & Simon 2005), rho Ophiuchus (M. Smith, et al. 2005), Serpens (Testi et al. 2000), LMC OB association LH 5 (Heydari-Malayeri et al. 2001), and W51 (Nanda Kumar, Kamath, & Davis, 2004). Very small stellar systems, consisting of only three or four stars inside a cluster, can also be hierarchical (e.g., Brandeker, Jayawardhana & Najita 2003). Numerical simulations showing this effect are in Bonnell, Bate & Vine (2003): stars appear to be born with a hierarchical distribution of sub-units. A stellar grouping presumably loses this structure only when the stellar ages become comparable to the cluster dynamical time, at which point the stars move away from their birth positions and mix together as a result of gravitational forces. We believe this is essentially the origin of star clusters: they are the inner mixed regions of a pervasive hierarchy of stellar birth positions resulting from gravitational fragmentation and turbulence.

In any hierarchically nested distribution, the number of units scales with mass as $M^{-2}dM$ because the same total mass is present at each logarithmic level in the hierarchy (a more general case is in Elmegreen 2002). Then $\beta = 2$ for the sub-units. In that case, the summed IMFs from all the sub-units in a cluster equals approximately the IMF of the

whole cluster. Otherwise, more massive clusters would have steeper IMFs, which is contrary to observations (e.g., Fig. 5 in Scalo 1998). Thus the equality between summed IMFs and individual IMFs is a common occurrence *inside* the cluster environment as it is outside the cluster environment, in whole galaxies. All of these regions are part of the hierarchy of star formation.

Numerical simulations of cluster formation suggest a far more complicated picture of how the IMF arises (see review in Bonnell, Larson, & Zinnecker 2006). Subclumps have their own mass segregation and their own enhanced accretion to the most central stars (Bonnell, Vine & Bate 2004). Then they blend together over time, with continued growth of the most massive stars. However, these processes appear to be a microcosm of what happens on larger scales: star clusters form clustered together, each with their own cloud core, mass segregation, and IMF, each accretes from the surrounding parts of the ISM, and they sometimes blend together over time into bigger clusters. Other times they blend into OB associations after locally dispersing. In either case, they add up to give about the same IMF in the composite region as they had individually. In terms of the physical processes at work, there is nothing random about this except for the smallest details in the initial conditions that get amplified by turbulence and self-gravity. Still, the basic equations for the distribution functions should be the same as in our simple models, as should the requirement that $\beta \sim 2$ to make the sum of all the IMF subunits equal to the observed IMF whole.

3. Observations of Galaxy-Integrated IMFs

The IMF for a galaxy is the sum of the IMFs of the individual star-forming regions and the IMFs of all the captured dwarfs and other extragalactic systems. This sum includes both field stars and the stars remaining in clusters. It cannot be observed directly using star counts unless the star formation history is known. This differs from the situation in globular clusters and other clusters where the stars presumably formed in a single burst. For galaxies, the integrated IMF may be determined, subject to certain assumptions, from broad-band colors, Hα equivalent widths, star counts of low-mass (unevolved) stars, and the relative abundances of various elements. Essentially all of the observations suggest the integrated IMF may be approximated by a power law at intermediate to high mass with a slope comparable to that of the Salpeter function ($dN/dM \propto M^{-\alpha}$ for $\alpha \sim 2.35$) or slightly steeper (e.g., $\alpha \sim -2.7$), and a flattening below a mass of ~ 1 M$_\odot$ or slightly less. Elliptical galaxies and clusters of galaxies may have formed with a slightly flatter IMF, which also appears to be characteristic of the Universe as a whole. Little is known about the integrated IMF below 0.1M$_\odot$. Here we review the recent observations of this summed IMF because

there is no comparable review in the literature.

For the local part of the Milky Way, star counts and metallicities suggest that the slope of the intermediate to high mass part of the IMF is comparable to or slightly steeper than the Salpeter slope (Scalo 1986; Rana 1987; Tsujimoto et al. 1997; Thomas, Greggio & Bender 1998; Boissier & Prantzos 1999; Gratton et al. 2000; de Donder & Vanbeveren 2003; Portinari et al. 2004). Carigi, et al. (2005) require an IMF slope of -2.7 to explain the C/H, N/H, and O/H ratios. This slope is somewhat difficult to constrain because it depends on the upper stellar mass limit, the star formation history, gas accretion rate, stellar migration, stellar evolution models, and other things.

In the Milky Way bulge, several of these uncertainties are not so important (e.g., age variations, migration). There, the integrated IMF for $0.15 < M/\mathrm{M}_\odot < 1$ is similar to that of globular clusters (Holtzman et al. 1998; Zoccali et al. 2000). The galaxy-wide IMF in the local dwarf Spheroidal Ursa Minor is also indistinguishable from the IMFs of Milky Way globular clusters (Feltzing, Gilmore & Wyse 1999). Similarly, the IMF in the Draco Dwarf Spheroidal is like that in the old cluster M68 (Grillmair et al. 1998). If stars typically form in clusters that subsequently disperse to make a bulge or a dwarf galaxy, then these three examples suggest directly that the summed IMF from a population of clusters approximately equals the IMF of each cluster.

Other nearby dwarf and Irregular galaxies have IMFs with slopes similar to the Salpeter value. Crone et al. (2002) find from models of color-magnitude diagrams that the IMF in the BCD galaxy UGCA 290 is approximately Salpeter for intermediate mass stars; a slope as steep as -3 overproduces the faint blue main sequence relative to the brightest supergiants. Annibali et al. (2003) determined the range of acceptable IMFs from color-magnitude models for NGC 1705. In Region 7 of that galaxy, the Salpeter slope or slightly flatter ($\alpha = -2.35$ to -2) for $M > 6$ $\mathrm{M}_\odot$ gave an acceptable fit – one steeper produced a luminosity function that was too steep for the most recent burst. In Region 6 of NGC 1705, the preferred IMF slope was Salpeter or possibly steeper, with a limit at about -2.6. The dwarf irregulars DDO 210 and DDO 3109 have approximately Salpeter IMFs at intermediate mass as well (Greggio et al. 1993). In NGC 1309, a slightly shallower IMF was preferred (-2.2) to match the observed proportion of main sequence stars to evolved stars; a steeper IMF, including even the Salpeter IMF, overproduced evolved stars with moderate mass. NGC 1569, a starbursting dwarf, the IMF was Salpeter or slightly flatter (Angeretti et al. 2005), as it was in NGC 6822 (Marconi et al. 1995). NGC 6822 was also studied more recently by Carigi, Colín & Peimbert (2005) using models of chemical evolution. Reasonable results were obtained with the Kroupa, Tout & Gilmore (1993) IMF, which has a slope at intermediate to high mass of -2.7. They suggest, however, that the upper limit to the stellar mass should be lower than

in Kroupa, Tout & Gilmore, namely ~ 60 $M_\odot$ rather than 80 $M_\odot$.

The IMFs in Wolf-Rayet galaxies were studied by Fernandes et al. (2004) using the ratio of Wolf-Rayet stars to O-type stars obtained from spectra. The low metallicity galaxies of this type were fitted to an IMF with a slope between -2 and -2.35 in a short burst of star formation. The high metallicity galaxies were found to have either a steeper slope in the bursting models, or the Salpeter slope (-2.35) in more extended bursts. However, the ratio of Carbon to Nitrogen Wolf Rayet stars supported the extended burst models. Thus the preferred IMFs were never steeper than the Salpeter slope in that study.

These observations of dwarf galaxies support the proposal outlined in the Introduction that the IMF from each cluster equals approximately the IMF of the whole stellar population. This contradicts the basic proposal about summed IMFs in Kroupa & Weidner (2003), and it also contradicts the models in Weidner & Kroupa (2005) which suggest that small galaxies should have steeper IMFs than large galaxies. The basis for Weidner & Kroupa's 2005 model was that smaller galaxies, with very low star formation rates, should have a small number clusters and therefore a small mass for the most massive cluster, from statistical sampling. Then, if the maximum stellar mass depends on the cluster mass, the formation of high mass stars should be relatively rare. However, even dwarf galaxies can contain super star cluster with very massive stars in them (Billett, Hunter, & Elmegreen 2002). Massey, Johnson, & Degioia-Eastwood (1995) also noted that the maximum masses for stars are about the same in the Milky Way, the LMC and the SMC, despite the size differences among these three galaxies.

One exception to the near uniformity of IMF slopes for dwarf galaxies is in the main body of the BCD galaxy I Zw 18, which apparently has a flat IMF with a slope of ~ -1.5 (Aloisi, Tosi, & Greggio 1999). This conclusion was based on color-magnitude diagrams obtained with the Hubble Space Telescope and is clearly different from that in all of the other dwarfs studied by this group using the same methods. The origin of this discrepancy has not been explained, but in any case, the observed slope is not steeper than the nominal cluster IMF.

The IMF in the Large Magellanic Cloud has been determined for many regions. Holtzman et al. (1997) observed a field region for stars between ~ 0.6 $M_\odot$ and 1.1 $M_\odot$ and derived an IMF slope between -2.0 and -3.1. Parker et al. (1998) determined IMFs slopes for massive stars in field regions and got -2.80 ± 0.09. Selman & Melnick (2005) observed the LMC field outside the star formation regions near 30 Dor and found an IMF slope of -2.38 ± 0.04 for $7 < M/M_\odot < 40$. This is essentially the same as the Salpeter IMF. Selman & Melnick pointed out that this field slope is slightly steeper (by 0.12) than the IMF in the nearby super star cluster, NGC 2070, in agreement with predictions about field-star IMF

steepening by Kroupa & Weidner (2003) for $\beta = 2$. Higher β would not give this result. Steeper field IMFs for the LMC will be discussed below.

Large galaxies have integrated IMF slopes comparable to the Salpeter value. Fifty OB associations summed together in M31 were found to have an IMF slope of -2.59 ± 0.09 using a combination of space-based uv and HST photometry, 2MASS photometry at JHK bands, and I band photometry (Veltchev, Nedialkov, & Borisov 2004). The stellar masses ranged from 8 $M_\odot$ to 100 $M_\odot$. Kennicutt and collaborators measured the integrated IMFs in several hundred nearby galaxies of various Hubble types using optical and Hα surface brightnesses (Kennicutt 1983; Kennicutt, Tamblyn & Congdon 1994; Bresolin & Kennicutt 1997; Bresolin et al. 1998). The IMF did not vary with Hubble type or galaxy luminosity, and was usually fit with a power law at intermediate to high mass with a slope of ~ -2.5.

The summed IMF for all of the stars in clusters of galaxies has been studied in detail using constraints from broad-band colors and the metallicities of the galaxies and the intergalactic medium. Metallicity is sensitive to the mass fraction of high mass stars and α abundance ratios are sensitive to the ratio of intermediate to high mass stars. The general consensus seem to be that the IMFs in galaxy clusters had to be flatter than Salpeter at some time in the past, when the metallicity of the intergalactic medium was established. Then it probably steepened to the Salpeter slope in recent times. Renzini et al. (1993) fit the Fe abundance in clusters with a Salpeter IMF in the quiescent star forming phases and a flatter IMF in the bursts. Loewenstein & Mushotsky (1996) fitted elemental abundances in four rich clusters of galaxies with an IMF flatter than Salpeter (the suggested slope was in the range -1.7 to -2 to get enough Fe). Chiosi (2000) suggested the characteristic (turnover) mass in the IMF got larger with redshift, as did Moretti, Portinari, & Chiosi (2003), who fitted the intra-cluster metallicities with proportionally more massive stars at high redshift and in more massive galaxies. Tornatore et al (2004), Romeo et al. (2004), Portinari et al. (2004), and Nagashima et al. (2005a) also suggested the intra-cluster abundances came from a top-heavy IMF in the past, particularly in the most massive and most bursting galaxies. Pipino & Matteucci (2004) and Nagashima et al. (2005b) suggested a slightly top-heavy IMF for massive elliptical galaxies. All of these studies concluded that the composite IMF was Salpeter or slightly flatter than Salpeter when galaxy clusters formed. Still, a Salpeter IMF may be possible if a significant fraction of intra-cluster Fe comes from Type II supernovae (Wyse 1997). Simulated color-magnitude diagrams of ground-based U,V observations of the nearby elliptical galaxy NGC 5128 suggest a Salpeter IMF, with a limit no steeper than -2.6 (Rejkuba, Greggio & Zoccali 2004). There is no evidence that the integrated IMFs in galaxy clusters are significantly steeper than Salpeter, even though galaxies and clusters of galaxies formed from the sum of countless dispersed star clusters.

On a larger scale, Baldry & Glazebrook (2003) fitted the local luminosity density and star formation history of the Universe with population synthesis models and obtained an average IMF slope of -2.15 ± 0.2 for all galaxies combined. The upper limit to the slope was -2.7. Lacey et al. (2005) modelled galaxy formation and matched the observed UV galaxy luminosity function over a wide range of redshifts with a solar neighborhood IMF that becomes top-heavy in starbursts. Calura & Matteucci (2004) fitted the relative abundance of elements in galaxies of various types and found the Salpeter IMF was the best choice for a universal IMF.

Evidently, most observations of galaxies suggest the composite IMF is not significantly steeper than the Salpeter IMF, even though these systems are the combinations of many small clusters and associations, each of which probably has the Salpeter IMF on average, like local clusters and associations. There is no systematic steepening of the IMF in composite fields.

Nevertheless, several observations suggest the IMF in some regions is significantly steeper than the Salpeter slope. Gouliermis, Brandner & Henning (2005) measured the IMF in a field region near the giant shell LMC4. They obtained a slope of ~ -6 for $0.9 < M/\mathrm{M}_\odot < 2$ and ~ -3.6 for $0.9 < M/\mathrm{M}_\odot < 6$. These slopes at low mass agree with those found by Massey (2002) for high mass stars. There are other galaxies where steep IMFs have been reported. The high mass-to-light ratio in the disks of low surface brightness galaxies was taken as evidence for an IMF slope of -3.85 by Lee et al. (2004). Also, Zackrisson, et al. (2004) suggested that the IMF slope is -4.5 in the red stellar halos around BCD galaxies (Bergvall & Östlin 2002) and in the red halos of stacked images of edge-on disks (Zibetti, White & Brinkmann 2004). These steep slopes can be explained by the Kroupa & Weidner (2003) model with $\beta > 2.3$, but there are other explanations for steep slopes in these particular regions also (Elmegreen 2004; Elmegreen & Scalo 2006).

4. Monte Carlo Models

The difference between the IMF of a single cluster and the summed IMFs of many clusters can be seen from Monte Carlo simulations where star and cluster masses are randomly chosen from distribution functions (e.g., Weidner & Kroupa 2003, 2005, 2006). This is only an approximation meant to simulate the diverse processes happening in the cluster environment. Cluster simulations suggest a correlation between cluster mass and star mass, possibly because of definite physical processes (e.g., Bonnell, Vine & Bate 2004). These are likely to produce interesting variations around the average condition, some of which may correlate with environment in ways that are not considered by these simple models. Still, after real clusters disperse and the stars mix with other dispersed stars, the summed IMF

should depend on the cluster mass function in the manner suggested by these simple models, and it should depend on the range of cluster mass where each star is likely to form.

Here we discuss Monte Carlo calculations like those in Weidner & Kroupa, but with an important difference. We select a cloud mass from a mass distribution function and then select stars until the total stellar mass exceeds an efficiency factor ϵ times the cloud mass. This has the same effect of building up clusters with a pre-set cluster mass function (equal to the cloud mass function), but the rejection of stars is soft. This difference is important because when stars build up in a cloud core, their feedback on the gas gets stronger until the gas is expelled and star formation stops. There should not be a sudden point at which all star formation stops, but a gradual transition. During this transition, it is likely that low mass stars continue to form, as there is generally a lot of gas left over in the cloudy debris. There may not be enough gas to form high mass stars though. In the simulation, we include in the cluster any selected star that fits in the remaining gas reservoir, and then stop the selection process after the efficiency exceeds the assumed value. This procedure differs significantly from that in Weidner & Kroupa (2003, 2005) for low mass stars. Weidner & Kroupa stopped the selection process when the total stellar mass exceeded the pre-set cluster mass, without regard to the mass of the final excluded star. Thus their exclusion process operated on stars of all masses, and their summed IMFs in the $\beta > 2$ cases were steeper for all masses. Our exclusion process operates only on stars more massive than $1 - \epsilon$ times the cloud mass, so our summed IMF is steepened only for stars more massive than $(1 - \epsilon)$ times the minimum cloud mass. If stellar clustering continues all the way down to single stars (Kiss et al. 2006), then this difference is not important. But if star clusters have a minimum mass of ~ 30 $M_\odot$ (Lada & Lada 2003), then the difference in these two methods is important regardless of β. We use this procedure to illustrate a second way in which the summed IMFs in galaxies can be comparable to the individual cluster IMFs, distinct from the condition mentioned previously that $\beta \sim 2$. However, even without this assumption it will be clear from the high mass part of the Monte Carlo IMF that the $\beta \leq 2$ case gives a summed IMF indistinguishable from the individual IMF.

Our model stellar IMF is a power law at intermediate to high mass with a generic slope of -2.5, i.e., close to the Salpeter value of -2.35 but not intended to match any particular observation. The IMF turns over at the mass $M_t = 0.5$ $M_\odot$ and rises as M^{-1} below that (i.e., it becomes flat on a log-log plot):

$$n(M_s)dM_s = n_{0s} M^{-2.5} \left(1 - e^{-[M/M_t]^{1.5}}\right) dM_s. \tag{9}$$

Clusters are considered to form inside gas clouds with an efficiency ϵ. The cloud mass

function is a power law proportional to the final cluster mass function:

$$n_{cld}\left(M_{cld}\right) dM_{cld} = n_{0,cld} M_{cld}^{-\beta} dM_{cld}. \tag{10}$$

Here M_{cld} represents a cloud mass. The average stellar mass inside each cloud is $M_{cl} = \epsilon M_{cld}$. The efficiency is constant for each cluster in the summed IMF, so the final cluster mass distribution is the same power law as the cloud distribution.

The lower and upper mass limits to the IMF are taken to be $M_{min} = 0.01$ $M_\odot$ and $M_{max} = 150$ $M_\odot$ (following Weidner & Kroupa 2004; Oey & Clarke 2005; Koen 2006). For clouds, $M_{cld,min} = 10$ $M_\odot$ or 1 $M_\odot$ in two cases, and $M_{cld,max} = 10^6$ $M_\odot$. The lower limit to the cloud mass will have an effect on the summed IMF, but the upper limit is sufficiently high that sampling rarely selects such a massive cloud, and its effect is small.

The selection process works as follows. First a cloud mass M_{cld} is randomly chosen from the distribution function n_{cld} and then stellar masses M are randomly chosen for this cloud from $n_s(M)$. The running sum of stellar masses in this cloud is Σ_M. The remaining mass available for more stars is $M_{cld} - \Sigma_M$. If the most recent star chosen has a mass less than $M_{cld} - \Sigma_M$, then there is room for it in the cloud and it is added to the list of cluster stars. If the most recent star has a mass exceeding this value, then the star is not kept and another star is chosen. This is how stars are rejected. When the running sum exceeds ϵM_{cld}, the selection of stars for that cloud ends and another model cloud is chosen. We continue in this way until the total number of stars in all clusters is 10^8.

We are interested in the summed stellar mass distribution from all of the clusters, the summed IMF of the rejected stars, and the dependence of maximum stellar mass on cloud mass. For this latter quantity, we evaluate both the average maximum stellar mass for clouds within a range of values, and the absolute maximum stellar mass ever chosen for a particular cloud mass range. For the first quantity we find the maximum stellar mass for all clouds in a range of cloud masses and average these maxima together. This average is always less than the second quantity, which is the absolute maximum stellar mass found in the same clusters. We showed in Section 2 that the average maximum stellar mass per cluster increases in direct proportion to the cluster mass, independent of β, whereas the absolute maximum stellar mass for many clusters within a range of cluster masses is independent of cluster mass when $\beta = 2$.

Figure 1 shows these quantities for $\beta = 2$ and $\epsilon = 0.1$, 0.3, and 0.9. In the bottom panel, the lower of the two parallel curves is the individual cluster IMF from equation 9 (with arbitrary vertical shift). The upper curve is actually three curves superposed that show the summed IMFs for the three values of ϵ; they overlap nearly exactly. The bottom three curves are the mass functions for the rejected stars (which are not necessarily the last

stars chosen in a cluster). The top panel shows the theoretical prediction for the average maximum stellar mass versus cluster mass, obtained by numerical integration over equation 9. Other curves are the Monte Carlo results for maximum star mass labelled by ϵ. The smallest cloud mass is 10 $M_\odot$ in these models, so the smallest cluster masses are 1, 3, and 9 $M_\odot$ after multiplying by ϵ. Also shown in the top panel is the absolute maximum stellar mass for factor-of-ten intervals in cluster mass (the plus, cross, and circle marks). The line marked "$\epsilon\times$Cloud Mass" is the nominal cluster mass. The absolute maximum stellar mass exceeds the nominal cluster mass in low-mass clouds when a massive star is chosen early, before numerous low mass stars deplete the cloud mass. The absolute maximum stellar mass cannot exceed the cloud mass.

Figure 1 shows that the summed IMF is barely steeper than the cluster IMF for $\beta = 2$. The difference in slope is ~ 0.1 for $M > 10$ $M_\odot$. The efficiency ϵ does not matter much for this result. Only high mass stars are rejected, $M > (1 - \epsilon)\, M_{cld}$ for $M_{cld} = 10$ $M_\odot$. In the top panel, the average maximum stellar mass follows the prediction, as does the absolute maximum, which is about constant except for the lowest-mass clusters. This constancy is the primary reason why the summed IMF is so similar to the individual IMF even when there are far more low mass clusters than high mass clusters. The *average* maximum stellar mass per cluster increases with cluster mass, but the *absolute* maximum stellar mass does not except at very low M_{cld}.

Figure 2 shows the summed IMFs in the middle panel, the rejected IMFs in the bottom panel, and the cluster mass functions in the top panel for four values of β, a minimum cloud mass of 10 $M_\odot$, and $\epsilon = 0.3$. Also shown in the bottom two panels is a case with $M_{cld,min} = 1$ $M_\odot$, $\beta = 3$, and $\epsilon = 0.3$ (dashed lines), and another case with $M_{cld,min} = 10$ $M_\odot$, $\beta = 3$, and $\epsilon = 0.99$ (dotted lines). The first shows the effect of minimum cloud mass, which determines the point in the summed IMF where the steep slope begins. The second shows the effect of efficiency ϵ. When the slope of the summed IMF is steep, the number of rejected stars is large, even comparable to the total number of stars in the $\beta = 2$ case. Note, however, that when $\beta \leq 2$, the fraction of stars that are rejected is small for all stellar masses, $< 20\%$, as shown also in the bottom of Figure 1. This is why the summed IMF is about the same as the individual cluster IMF for small β. That is, stars with masses comparable to or larger than the cloud mass are rejected, but their number is negligible compared to the number of stars that are kept.

The bottom two panels of Figure 2 show how the slope of the summed IMF follows the slope of the cluster mass function. This dependence may be seen from solutions to equation 4. Least squares fits to the summed IMF slopes above 10 $M_\odot$ in Figure 2 give values of -1.5, -1.6, -2.1, and -2.6 for $\beta = 1.5$, 2, 2.5, and 3 when $M_{cld,min} = 10$ $M_\odot$ and $\epsilon = 0.3$. When

$M_{cld,min} = 1$ $M_\odot$, $\beta = 3$, and $\epsilon = 0.3$ (dashed curve), the slope is -2.8 above 1 $M_\odot$. When $M_{cld,min} = 10$ $M_\odot$, $\beta = 3$, and $\epsilon = 0.99$ (dotted curve), the slope is -2.5 above 10 $M_\odot$. The scatter in these slopes is on the order of ± 0.05.

The figures confirm the analytical results of Section 2 that the summed IMF from a population of clusters is indistinguishable from the individual cluster IMF when $\beta \leq 2$. The absolute maximum stellar mass is independent of the cluster mass even though the average maximum stellar mass increases with cluster mass. These results follow from the model because the fraction of stars that are rejected is negligibly small in the $\beta \leq 2$ cases.

5. Conclusions

Observations indicate that galactic bulges, whole galaxies of various types, clusters of galaxies, and the combined populations of stars in the Universe, all have composite IMFs with a slope close to the Salpeter value. The IMF appears to be slightly steeper than this in the Solar neighborhood and in a few other regions, and to have been slightly flatter in the past in massive or star-bursting galaxies that populate galactic clusters. Significantly steeper IMFs have been found in the field regions of the LMC and inferred from the colors and luminous densities of Low Surface Brightness galaxies and edge-on galaxy halos. For most galaxies, however, there is no evidence that composite IMFs are significantly steeper than individual IMFs observed in clusters and OB associations. If most stars form in such clusters and associations, then this near-equality of IMFs implies that the cluster and association mass distribution function is close to a power law with a negative slope of $\beta = 2$ for linear intervals of mass.

Stars form with no apparent physical connection between their mass and the resulting cluster mass. There is a statistical connection from the size of sample effect, with more massive clusters forming more massive stars on average, but this statistical connection has no obvious influence on the summed IMF from many clusters when $\beta = 2$. The probability that random sampling attempts to produce a star more massive than a cloud is negligible for $\beta = 2$. There is no correlation between the maximum stellar mass in a collection of similar clusters and either the cluster mass or the maximum average mass per cluster. Thus 100 Taurus-size clouds should be able to produce the same maximum stellar mass and the same IMF overall as a single cloud with 100 times the mass (regardless of β). This was shown analytically in Section 2 and with Monte Carlo simulations in Figure 1. The prediction has not been confirmed observationally, but such a confirmation could be subtle. The Orion cloud, for example, should appear to be composed of 100 Taurus-like smaller clouds when the density distribution is viewed with sufficiently high resolution and sensitivity.

These results fit in well with a model in which all clouds and young stars form in hierarchical patterns. Observations of many types suggest these patterns extend from kpc scales down to the scale of individual clusters. There is also tentative evidence for a continuation down to individual stars when the cluster environment has not mixed the stars together. In that case, neither clusters nor clouds are well-defined entities. They are defined more by observational selection and the dynamical processes following star formation than by the physics of individual star formation, which operates even in the pre-mixed cluster sub-units. What we perceive to be a cluster is most likely the mixed inner region of the hierarchy of young stars, with a size given by the approximate equality between dynamical time and age. In such a model, $\beta = 2$ automatically and stars are not limited by pre-defined cluster masses because there is no such thing as a pre-defined cluster.

REFERENCES

Aloisi, A. Tosi, M., & Greggio, L. 1999, AJ, 118, 302

Angeretti, L., Tosi, M., Greggio, L., Sabbi, E., Aloisi, A., & Leitherer, C. 2005, AJ, 129, 2203

Annibali, F., Greggio, L., Tosi, M., Aloisi, A., & Leitherer, C. 2003, AJ, 126, 2752

Baldry, I.K., & Glazebrook, K. 2003, ApJ, 593, 258

Bergvall, N., & Östlin, G. 2002, A&A, 347, 556

Bica, E., Claria, J. J., Dottori, H., Santos, J. F. C., Jr., & Piatti, A. E. 1996, ApJS, 102, 57

Bica, E., L. D., Schmitt, H. R., Dutra, C. M., & Oliveira, H. L. 1999, AJ, 117, 238

Billett, O.H., Hunter, D.A., & Elmegreen, D.M. 2002, AJ, 123, 1454

Boissier S., & Prantzos N., 1999, MNRAS, 307, 857

Bonnell, I. A., Bate, M. R., & Vine, S. G. 2003, MNRAS, 343, 413

Bonnell, I. A., Vine, S. G., & Bate, M. R. 2004, MNRAS, 349, 735

Bonnell, I.A., Larson, R.B., & Zinnecker, H. 2006, Protostars and Planets V, in press

Brandeker, A., Jayawardhana, R., & Najita, J. 2003, AJ, 126, 2009

Bresolin, F., & Kennicutt, R. C., Jr. 1997, AJ, 113, 975

Bresolin, F., Kennicutt, R. C., Ferrarese, L., et al. 1998, AJ, 116, 119

Calura, F., & Matteucci, F. 2004, MNRAS, 350, 351

Carigi, L., Colín, P., & Peimbert, M. 2005, astroph/0509829

Carigi, L., Peimbert, M., Esteban, C., & Garcia-Rojas, J. 2005, ApJ, 623, 213

Chabrier, G. 2003, PASP, 115, 763

Chiosi, C. 2000, A&A, 364, 423

Crone, M.M., Schulte-Ladbeck, R.E., Greggio, L., & Hopp, U. 2002, ApJ, 567, 258

Dahm, S. E., & Simon, T. 2005, AJ, 129, 829

de Donder, E., & Vanbeveren, D. 2003, NewA, 8, 415

de Grijs, R., Anders, P., Bastian, N., et al. 2003, MNRAS, 343, 1285

de Grijs, R. & Anders, P. 2006, MNRAS, 366, 295

Elmegreen, B.G. 2000, in Star formation from the small to the large scale, ed. F. Favata, A. Kaas, and A. Wilson. Noordwijk: European Space Agency, ESA SP 445, p.265

Elmegreen, B.G. 2001, in From Darkness to Light: Origin and Evolution of Young Stellar Clusters, ed. T. Montmerle and P. André, ASP Conference Proceedings, Vol. 243 San Francisco: Astronomical Society of the Pacific, p.255

Elmegreen, B.G. 2002, ApJ, 564, 773

Elmegreen, B.G. 2004, MNRAS, 354, 367

Elmegreen, B.G., & Efremov, Yu. N. 1997, ApJ, 480, 235

Elmegreen, B.G., Elmegreen, D.M., Chandar, R., Whitmore, B.,& Regan, M. 2006, ApJ, submitted

Elmegreen, B.G., & Scalo, J. 2006, ApJ, 636, 149

Feltzing, S., Gilmore, G., & Wyse, R.F.G. 1999, ApJL, 516, 17

Fernandes, I.F., de Carvalho, R., Contini, T., & Gal, R.R. 2004, MNRAS, 355, 728

Gieles, M., Larsen, S. S., Scheepmaker, R. A., Bastian, N., Haas, M. R., & Lamers, H. J. G. L. M. 2006, A&A, 446, L9

Gouliermis, D., Brandner, W., & Henning, Th. 2005, ApJ, 623, 846

Gomez, M., Hartmann, L., Kenyon, S. J., & Hewett, R. 1993, AJ, 105, 1927

Goodwin, S.P., & Pagel, B.E.J. 2005, MNRAS, 359, 707

Gratton, R. G., Carretta, E., Matteucci, F., & Sneden, C. 2000, A&A, 358, 671

Greggio, L., Marconi, G., Tosi, M., & Focardi, P. 1993, AJ, 105, 894

Grillmair, C.J., et al. 1998, AJ, 115, 144

Heydari-Malayeri, M., Charmandaris, V., Deharveng, L., Rosa, M.R., Schaerer, D., & Zinnecker, H. 2001, A&A, 372, 495

Holtzman, J.A., Mould, J.R., Gallagher, J.S., III, et al. 1997, AJ, 113, 656

Holtzman, J. A., Watson, A. M., Baum, W.A., Grillmair, C.J., Groth, E.J., Light, R.M., Lynds, R., O'Neil, E.J., Jr. 1998, AJ, 115, 1946

Hunter D. A., Elmegreen B. G., Dupuy T. J., & Mortonson M., 2003, AJ, 126, 1836

Kennicutt, R.C., Jr. 1983, ApJ, 272, 54

Kennicutt, R.C., Jr., Tamblyn, P., & Congdon, C.W. 1994, ApJ, 435, 22

Kiss, Z.T., Tóth, L.V., Ward-Thompson, D., Elmegreen, B., Balázs, L.G., Könyves, V., Ács, B., & Klagyvik, P. 2006, A&A, submitted

Koen, C. 2006, MNRAS, 365, 590

Kroupa, P., Tout, C.A., & Gilmore, G. 1993, MNRAS, 262, 545

Kroupa, P., & Weidner, C. 2003, ApJ, 598, 1076.

Lada, C.J., & Lada, E.A. 2003, ARAA, 41, 57

Larsen, S.S. 2002, AJ, 124, 1393

Lee, H.-C., Gibson, B.K., Flynn, C., Kawata, D., & Beasley, M.A. 2004, MNRAS, 353, 113

Loewenstein, M., & Mushotsky, R.F. 1996, ApJ, 466, 695

Marconi, G., Tosi, M., Greggio, L., & Focardi, P. 1995, AJ, 109, 173

Massey, P., Johnson, K.E., & Degioia-Eastwood, K. 1995, ApJ, 454, 151

Massey, P. 2002, ApJS, 141, 81

Moretti, A., Portinari, L., & Chiosi, C. 2003, A&A, 408, 431

Nagashima, M., Lacey, C. G., Baugh, C.M., Frenk, C.S., & Cole, S. 2005a, MNRAS, 363, 1247

Nagashima, M., Lacey, C. G., Okamoto, T., Baugh, C.M., Frenk, C.S., & Cole, S. 2005b, MNRAS, 363, L31

Nanda Kumar, M.S., Kamath, U.S., & Davis, C.J. 2004, MNRAS, 353, 1025

Oey, M.S., & Clarke, C.J. 2005, ApJL, 620, 43

Pipino, A., & Matteucci, F. 2004, MNRAS, 347, 968

Portinari, L., Moretti, A., Chiosi, C., & Sommer-Larsen, J. 2004a, ApJ, 604, 579

Rana, N.C. 1987, A&A, 184, 104

Rejkuba, M., Greggio, L., & Zoccali, M. 2004, A&A, 415, 915

Renzini, A., Ciotti, L., D'Ercole, A., & Pellegrini, S. 1993, ApJ, 419, 52

Romeo, A.D., Sommer-Larsen, J., Portinari, L., & Antonuccio-Delogu, V. 2004, MNRAS, in press, astroph/0509504

Scalo J.M., 1986, Fund. Cosmic Phys., 11, 1

Scalo, J. 1998, in The Stellar Initial Mass Function, ed. G. Gilmore, I. Parry, & S. Ryan (Cambridge: Cambridge Univ. Press), 201

Selman, F. & Melnick, J. 2005, A&A, 443, 851

Smith, M. D., Gredel, R., Khanzadyan, T., & Stankeinst, T. 2005, MmSAI, 76, 247

Testi, L., Sargent, A.I., Olmi, L., & Onello, J.S., 2000, ApJ, 540, L53

Thomas D., Greggio L., & Bender R., 1998, MNRAS, 296, 119

Tornatore, L., Borgani, S., Matteucci, F., Recchi, S., & Tozzi, P. 2004, MNRAS, 349, L19

Tsujimoto T., Yoshii Y., Nomoto K., Matteucci F., Thielemann F.K., & Hashimoto M., 1997, ApJ, 483, 228

Veltchev, T., Nedialkov, P., & Borisov, G. 2004, A&A, 426, 495

Weidner, C., Kroupa, P. & Larsen, S.S. 2004, MNRAS, 359, 1530

Weidner, C., & Kroupa, P. 2004, MNRAS, 348, 187

Weidner, C., & Kroupa, P. 2005, ApJ, 625, 754

Weidner, C. & Kroupa, P. 2006, MNRAS, 365, 1333

Wyse, R.F.G. 1997, ApJL, 490, 69

Zackrisson, E., Bergvall, N., Marquart, T., & Mattsson, L. 2004, astroph/0411537

Zhang, Q., & Fall, S.M. 1999, ApJL, 527, 81

Zibetti, S., White, S.D.M., & Brinkmann, J. 2004, MNRAS, 347, 556

Zoccali, M., Cassisi, S., Frogel, J.A., Gould, A., Ortolani, S., Renzini, A., Rich, R. M., & Stephens, A.W. 2000, ApJ, 530, 418

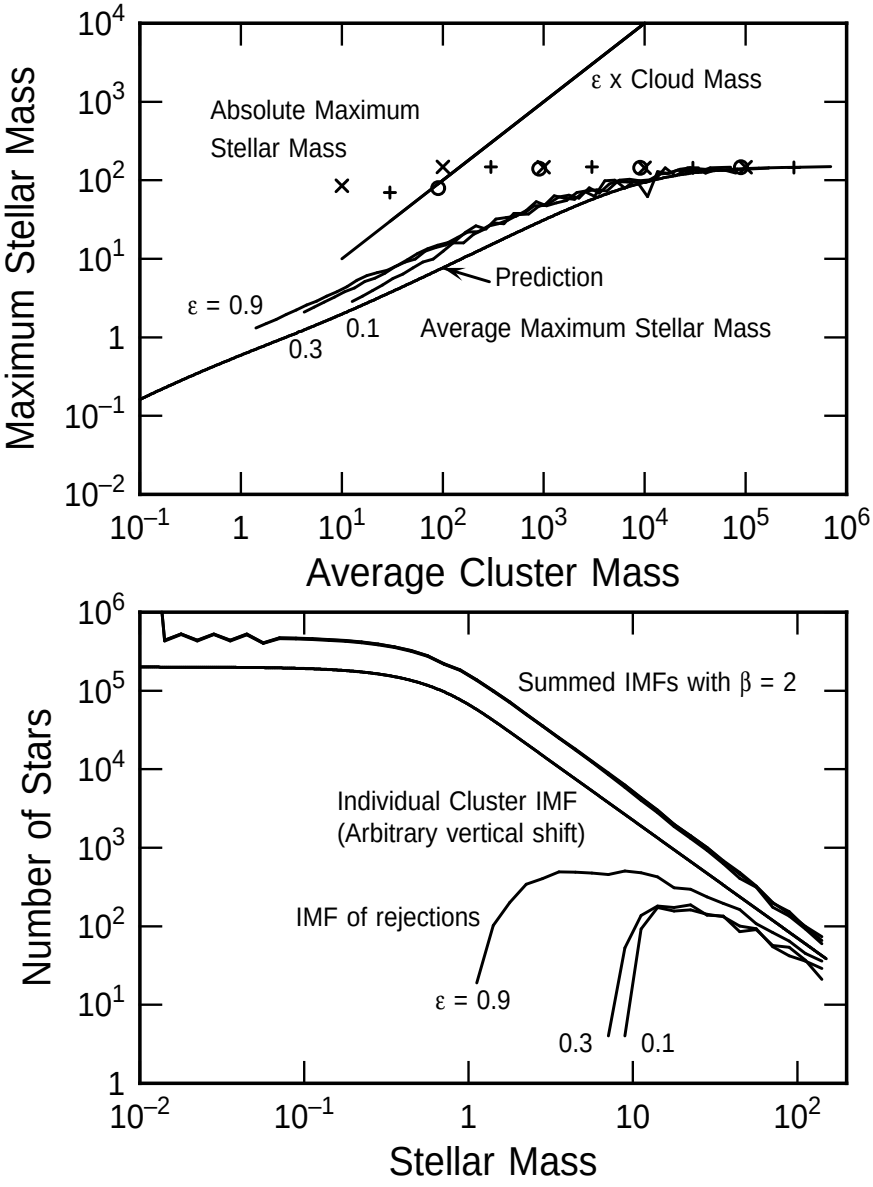

Fig. 1.— Monte Carlo IMF models with a cluster mass function slope $\beta = 2$. The bottom panel shows the individual cluster IMF that is input to the model, and it shows three summed IMFs for different star-formation efficiencies ϵ; these three summed IMFs are nearly identical to each other and their curves overlap. The IMFs of the rejected stars, which are those too massive to fit in the remaining gas of the cloud, are at the bottom. The top panel shows the correlation between the average maximum stellar mass in a cluster and the cluster mass (increasing curves). The absolute maximum stellar masses for all clusters, in bins spaced by a factor of 10 in cluster mass, are shown by symbols centered in their mass bins. The cases $\epsilon = 0.1$, 0.3, and 0.9 are represented by "x," plus, and circle. The summed IMF for this $\beta = 2$ case is nearly identical to the individual cluster IMF even though the average maximum stellar mass increases with cluster mass. This IMF similarity is the result of the near-constant absolute maximum stellar mass, which is a general property of power law cluster IMFs, and the $\beta = 2$ distribution for clusters.

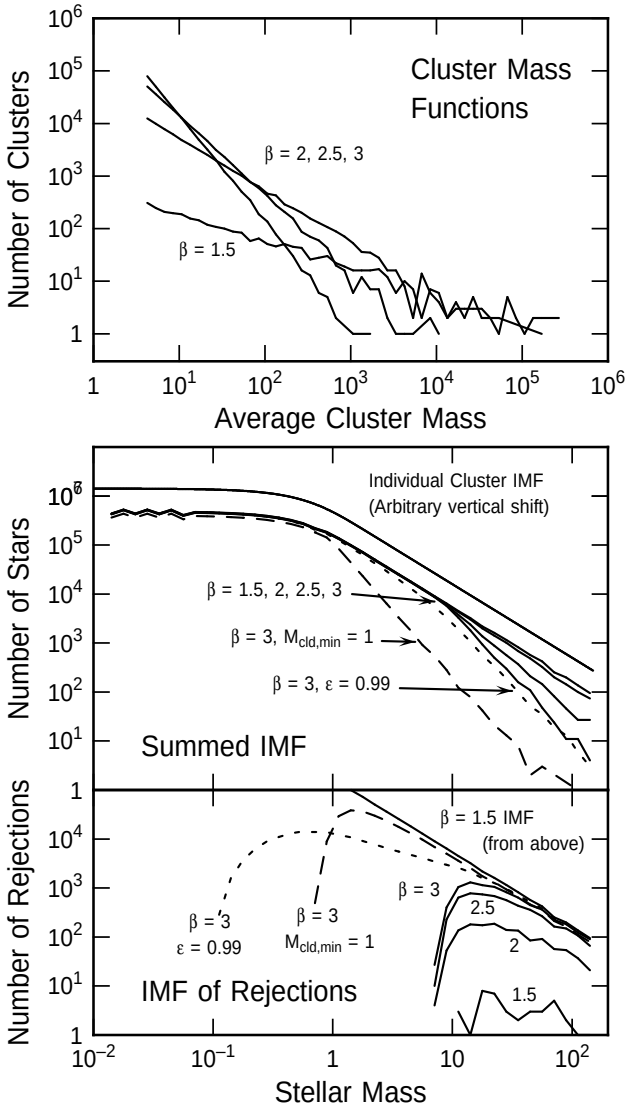

Fig. 2.— Summed IMFs for cluster populations with different cluster mass function slopes β. The minimum cloud mass is 10 $M_\odot$ for all curves except the one indicated, where it is 1 $M_\odot$. The star formation efficiency ϵ is 0.3 for all curves except the comparison case with $\epsilon = 0.99$. The summed IMF in the middle panel gets steeper with steeper cluster mass function, but agrees with the individual cluster IMF for $\beta \leq 2$. The summed IMF steepening begins at the minimum cloud mass for producing a cluster, depending slightly on ϵ. The bottom panel confirms that the rejection IMF becomes large at the stellar mass where the summed IMF begins to get steep. The randomly selected cluster mass functions used for these summed IMFs are shown in the top panel for the four cases with $\epsilon = 0.3$ and $M_{cld,min} = 10$ $M_\odot$. These cluster masses are on average ϵ times the cloud masses.